Energy contributions of different elastic moduli in mesh-based modeling of deformable objects*

Renáta Tóthová, Iveta Jančigová, Ivan Cimrák†
Cell-in-fluid Research Group
Faculty of Management Science and Informatics, University of Žilina
Univerzitná 8215/1, 010 26 Žilina, Slovakia
Email: {iveta.jancigova, renata.tothova, ivan.cimrak}@fri.uniza.sk

***Abstract*—To add**

I. Introduction

The modeling of flow with immersed objects gives important insights into various biological phenomena, e.g. propulsion of bacteria [1] or analysis of fish-like behavior [2]. Our current research is motivated by biomedical applications for which the simulation of blood on the level of blood cells immersed in a fluidic blood plasma is crucial. These applications, e.g. the design of microfluidic devices aimed for filtering of circulating tumor cells from blood [3], require the understanding of processes that depend on individual behavior of particular cells.

Biological cells, in particular red blood cells, are composed of two basic components: the cell membrane and the inner fluid. The membrane is elastic and its behavior is characterized by 5 different elastic moduli. The stretching modulus describes the shear resistance of the membrane, the bending modulus characterizes the bending resistance. Further, there is a local and global preservation of the surface and finally, the membrane preserves the volume of the red blood cell. All five moduli contribute to the elastic behavior of the cell, each modulus with different impact: sometimes the contribution from the stretching is significantly greater than that from the bending. The mutual weights of individual contributions can be tuned with elastic parameters k_s, k_b, k_a, k_A, and k_V. These symbols denote elastic parameters for stretching, bending, local area, global area and volume preservation, respectively.

In Figure 1 one can see the case when the stretching modulus is clearly dominating the area preservation moduli: the triangular network is being stretched in horizontal direction, the individual edges of the mesh are prolonged and the stretching modulus will be significant. On the other hand, the areas of individual triangles remain the same for both pictures and therefore the area preservation modulus vanishes.

In the example above, it is clear to guess which moduli are dominant and which are negligible. In more complex shapes however, this is not the case. Thus it is desirable to quantify the contribution of each elastic modulus to the overall elastic behavior. In this manuscript, we study several approaches how to measure the impact of each elastic modulus. We suggest a new approach based on the summation of the forces exerted on the individual mesh points.

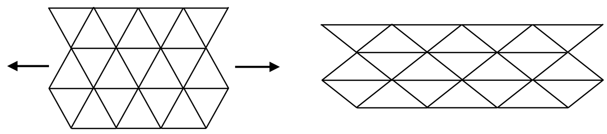

Fig. 1: An undeformed triangular network (left) is stretched with horizontal forces. Deformed network (right) where the areas of individual triangles remained the same as in the undeformed state, unlike the lengths of the individual edges. Consequently, the area preservation modulus vanishes, whereas the stretching modulus is significant.

Overview of the article: TO ADD

II. Model

A. Force calculations

The computational model for description of an elastic object is based on a triangular network covering the surface of the object. This is in agreement with the structure of the red blood cell, since it has the membrane and the inside filled with liquid. The network can be considered as a network of springs that exert forces on the network nodes. All forces are in some sense proportional to the deviation from the relaxed shape, which is a shape that the red blood cell has without any external forces. These forces then cause the changes of the object's shape and its movement in space, e.g. for the stretching, the force exerted on the endpoints of every edge in the mesh is proportional to the difference between the relaxed length of the edge and the stretched length. The actual expressions for evaluation of these forces may vary. We work with the following expressions that have been taken with some modifications from [4], [5]. For the ease of reading, we provide the expressions for the magnitudes of the forces only. The vectorial expressions can be found in [6]. Stretching force:

$$F_s = k_s(L - L_0) \tag{1}$$

where L is the relaxed length of the underlying edge of the mesh, and L_0 is the actual prolongation of this edge. Directions of the forces are along the edge. Bending force:

$$F_b = k_b \frac{\theta - \theta_0}{\theta_0} \tag{2}$$

*This work was supported by the Slovak Research and Development Agency under the contract No. APVV-0441-11.
† The work of Ivan Cimrák was supported by the Marie-Curie grant No. PCIG10-GA-2011-303580.

where θ is the resting angle between two triangles, and θ_0 is the deviation from this angle. Directions of the forces are perpendicular to corresponding triangles. Local area force:

$$F_a = k_a(S_\triangle - S_\triangle^0) \tag{3}$$

where $S_\triangle^0$ is the relaxed area of the triangle and $S_\triangle$ is the current area of the triangle. Directions of the forces are towards the centroid of the triangle. Global area force:

$$F_A = k_A \frac{S - S_0}{S_0} \tag{4}$$

where S is the current surface of the whole object and S_0 is the surface of the object in the relaxed state. Directions of the forces are again towards the centroid of the triangle. Volume force:

$$F_V = k_V \frac{V - V_0}{V_0} S_\triangle \tag{5}$$

where $S_\triangle$ is the area of the triangle V is the volume of the whole object, V is the relaxed volume. Directions of the forces are perpendicular to the triangle. Details of this model can be found in [7].

B. Energy of a spring system

When stretched, the network of springs stores energy U that is equivalent to the work needed to get the system from the relaxed state to the stretched state. In our case, the energy U consists of five different energies corresponding to five elastic moduli, so we have $U = U_s + U_b + U_a + U_A + U_V$. The individual forces are directly related to the energies, namely the force is the derivative of the energy with respect to the position $\mathbf{r}$. For example, we have

$$F_s = \frac{\partial U_s}{\partial \mathbf{r}}, \tag{6}$$

with analogous expressions for the other types of energy.

The knowledge of the previous expression suggests that its integration should give us the expressions for the energies, once we know expressions for the forces. This is however misleading. In the case of the stretching force and the stretching energy, the expression (1) is simple enough to derive the expression for the stretching energy of one edge

$$U_s = \frac{1}{2} k_s (L - L_0)^2. \tag{7}$$

The stretching energy of the whole triangular network will be the summation of (7) over all edges in the mesh.

The expressions (2)–(5) do not give straightforward expressions for the energies. Therefore one does not have the possibility to see the energy contribution when using (2)–(5).

Remark 1: There is an alternative approach. Instead of defining the forces and deriving the expressions for the energies, one can define the energies and derive the expressions for the forces. There are authors following this approach [8], [9]. We illustrate the disadvantage of this approach using the local area preservation modulus. The authors define the local preservation energy U_a^f

$$U_a^f = \frac{1}{2} k_a \frac{(S_\triangle - S_\triangle^0)^2}{S_\triangle^0}.$$

However, when one performs differentiation of the previous expression with respect to position, the directions of the resulting forces $F^f(a)$ are not towards the centroid of the triangle but perpendicular to the opposite side of the triangle. This results in extensive deformation of obtuse-angled triangles.

We thus conclude that the above approach is not optimal and can lead to unphysical mesh deformations.

III. $\mathcal{F}$-METRIC AS AN ALTERNATIVE TO ENERGY

Red blood cells are extremely elastic and they need to pass through narrow channels, e.g. microvessels in the blood circulation. To determine which parts of a red blood cell are exposed to the highest local stresses, one needs to measure the tensile stress in the membrane. Our model consists of five different moduli and each modulus contributes to the overall stress differently.

The elastic energies described in the previous sections represent one way of measuring the stress in the elastic membrane. However, we have seen that we do not possess the expressions for the computation of the energies. The numerical computation of the energies would involve tracking all forces from the relaxed state to the deformed state and their summation over the whole process. In simulations of physical objects, we mostly do not have the case that an object starts from the relaxed state and ends up in a deformed state. Usually, have the scenarios when the objects start in deformed states and further change their deformations.

Knowing this, we suggest a very simple metric how to compare the influence of different moduli. For each mesh point we will sum up all stretching contributions and the resulting force will be denoted by $\widetilde{\mathbf{F}}_s$. To be more specific, take one mesh point v with, e.g., five edges $e_1, \ldots, e_5$ attached to this point. From (1) we have five contributions of the stretching modulus that add forces to point v. Summing these five forces we get

$$\widetilde{\mathbf{F}}_s(v) = \sum_{i=1}^{5} \mathbf{F}_s(e_i)$$

where $\mathbf{F}_s(e_i)$ is the vectorial form of (1) evaluated for e_i.

Analogically, we can write similar expressions for the bending forces, etc. To sum up, for each point of the mesh we get an expression giving the information about of the forces coming from different elastic moduli acting on that particular mesh point.

To get an overall stretching modulus contribution to the whole object, we denote by $\mathcal{F}_s$ the sum of local point-wise contributions over all points in the mesh

$$\mathcal{F}_s = \sum_v \left| \widetilde{\mathbf{F}}_s(v) \right|.$$

Analogous expressions can be defined for all other elastic moduli.

We call this metric a $\mathcal{F}$-metric. To justify this, let us analyze the energy versus the $\mathcal{F}$-metric. The energy gives the information how much energy is stored in the current shape of the elastic object. However, for studies of the threshold values at which a membrane can rupture, the dynamics of the

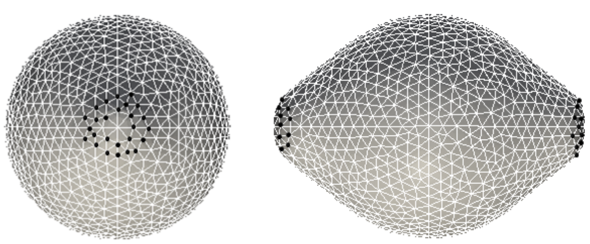

Fig. 2: Experiment A: the sphere is stretched by several mesh points located on a ring, indicated by black dots on two opposite sides. The force exerted on those points has horizontal direction.

stretching must be considered and therefore another important information is, how fast the energy changes. In other words, it is important to know the derivative of the energy, which leads us to look at the amount of force exerted on the individual points and the $\mathcal{F}$-metric gives us exactly this information.

IV. Comparison of elastic moduli using the $\mathcal{F}$-metric

We designed the following three experiments to illustrate the use of the $\mathcal{F}$-metric. In each experiment we deform an elastic object differently and we look at the $\mathcal{F}$-metric for different moduli. Each experiment is designed in a way that one particular modulus should have more impact than the others.

Simulations have been performed using the object-in-fluid framework [10] that our research group developed for simulations of objects (both elastic and stiff) moving in fluid. This framework is part of an open source molecular dynamics simulation package ESPResSo [11]. Visualizations have been done using open source analysis and visualization application ParaView [12].

Experiment A: Stretching of a sphere

We have used a triangulation of a sphere with $4\mu m$ radius and 1524 surface nodes. The sphere was immersed in stationary fluid that serves as a damping medium. The elastic parameters $k_s, \ldots, k_V$ were all set to 0.1. We decided to take the same value for all parameters in order to compare different $\mathcal{F}$-metrics. We applied a horizontal constant outward force at two opposite ends of the sphere. The force was equally distributed over several mesh points located on a ring with $0.2\mu m$ radius. These rings were perpendicular to the horizontal axis, see Figure 2.

To illustrate how the ratios between different $\mathcal{F}$-metrics can vary we used non-constant horizontal force. Namely, we divided the experiment into three stages, in stage one, the horizontal force was on, in stage two it was turned off and then again, in stage three we switched the horizontal force on. During such experiment we can see the elastic responses of the whole system to the changes of the horizontal stretching force.

In Figure 3 (a) we can see how the $\mathcal{F}$-metrics evolved. Surprisingly, the bending $\mathcal{F}_b$ has the largest values. This suggests that when we want to have approximately the same influence of all elastic moduli, we must set the elastic parameter k_b lower than others. This is also confirmed in the Expriment B, when the sphere radically deforms at 6 different locations.

From the scaled Figure 3 (b) one can see that the following four elastic moduli present the same behaviour: Bending, stretching, local and global area preservation. All four $\mathcal{F}$-metrics are cancavely increasing during the stage 1, after switching the horizontal force off, they radically convexly decrease, and in the stage three, after swithing the horizontal force again on, they concavely start increasing.

The volume preservation however has completely different evolution. First 2000 steps, the volume of the sphere increases and consequently, $\mathcal{F}_v$ increases. The transversal diameter of the sphere starts to shrink, which results in decrease of the volume, and eventually at around 6000 steps, the volume becomes the same as in the beginning which means that $\mathcal{F}_v$ vanishes.

Experiment B: 6-way poking of the sphere

In this experiment we have used the same sphere triangulation and the same set of elastic parameters as in Experiment A. The difference was in the applied forces. This time they did not point outward, but towards the center of the sphere. We have decided to apply the forces at six different areas of the sphere - "top", "bottom", "front", "back", "left" and "right". In each of these, the force acted at the pole and its eight neighbors, because we did not want to put too large amount of localized strain by acting on a single mesh point. The deformed sphere is depicted in Figure 4.

In this experiment we followed the same procedure as before - we first let the forces act on the object, then we turned them off and then we turned them on again. In Figure 5 we can see that the bending dominates $\mathcal{F}$-metrics in this experiment as expected - the angles between triangles have been changed significantly in the regions where the sphere was poked. Two other things to note about this chart are the following:

As before, while the stretching energy computed from formula 7 has significantly lower numerical values, the qualitative behavior corresponds to that of stretching $\mathcal{F}$-metrics. And secondly, looking at the formulas **??** and **??** it might seem that the global area conservation and volume conservation are very closely related and follow the same pattern, here it is clearly not the case. In the simulation experiment, the global area is increasing while the forces are turned on and the volume is decreasing. It is increasing when the forces are turned on. As a consequence, its $\mathcal{F}$-metrics curve does not have the same concave-convex-concave shape as the other metrics (except bending).

- something about the bending dip in the last third of the graph.

Experiment C: Inflating of a sphere

In this experiment we have used the same sphere triangulation and the same set of elastic parameters as in Experiments A and B. The exerted force was set in a such a way that it mimics inflating of the sphere. In each triangulation point the exerted force has the direction normal to the sphere. The deformation of the sphere is not interesting here since the inflated sphere remains a sphere. In this experiment we followed the same procedure as before - we first let the forces act on the object, then we turned them off and then we turned them on again.

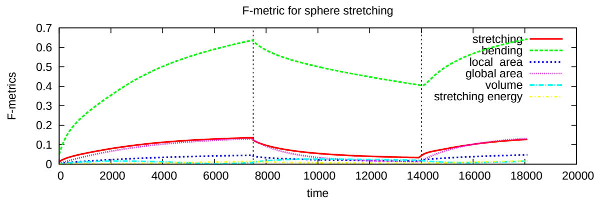

(a)

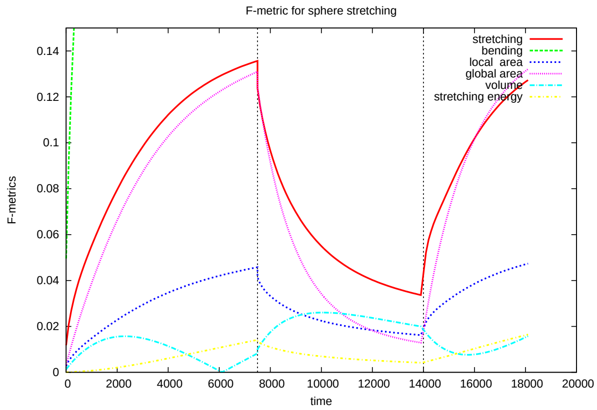

(b)

Fig. 3: Evolution of $\mathcal{F}$-metrics during the stretching sphere experiment. Two vertical dashed lines indicate the moments when the horizontal stretching force was switched off and then switched on again. (a) figure with all graphs visible, the significant difference is visible between $\mathcal{F}_b$ and all other $\mathcal{F}$-metrics, (b) scaled figure to see details without $\mathcal{F}_b$

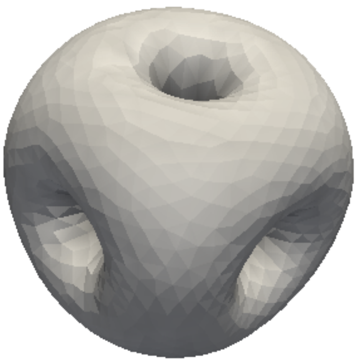

Fig. 4: Deformation of the sphere in Experiment B. Forces were applied at 6 different areas of the sphere towards its center.

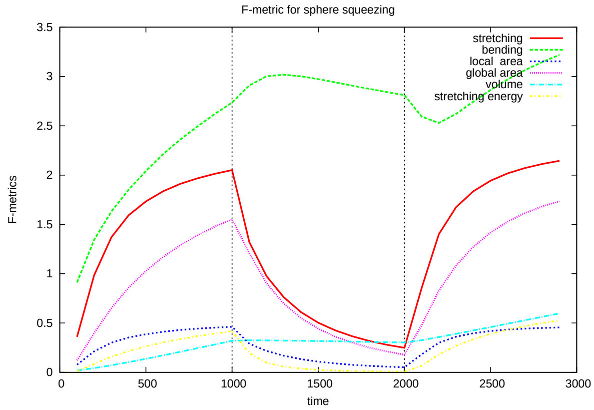

Fig. 5: Evolution of $\mathcal{F}$-metrics during Experiment B. Two vertical dashed lines indicate the moments when the horizontal stretching force was switched off and then switched on again.

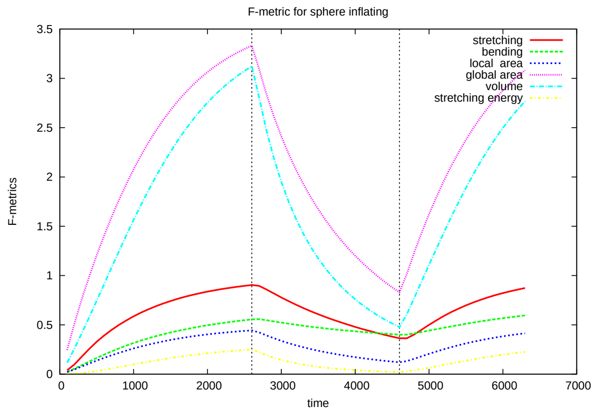

Fig. 6: To add

In the previous two experiments, $\mathcal{F}_b$ was dominating. In this experiment however we see that the bending plays much less important role. It is logical because when inflating sphere the inner angles between the triangles in the triangulation remain almost unchanged. Therefore there is no need to correct them. On contrary, the volume and global area changes significantly and this features we can see on the graph: Figure 6 demonstrates that $\mathcal{F}_A$ and $\mathcal{F}_V$ dominate over $\mathcal{F}$-metrics of other elastic moduli.

V. Conclusions

From all three experiments we see that the $\mathcal{F}_s$ copies the evolution of the stretching energy (yellow dot-dashed line in all graphs). The only difference is in the scaling factor. This justifies the use of $\mathcal{F}$-metric as an alternative to energy at least in the case of the stretching modulus.

The aim of the performed experiments was to show that

$\mathcal{F}$-metric is a suitable energy-like characteristic of action of elastic forces on the object. Indeed, in all experiments the graphs of $\mathcal{F}$-metrics corresponded to what we expected. Experiment A was designed to illustrate the main role of stretching and bending, which was cofirmed. Experiment B was designed to show the predominance of bending only, which was confirmed too. Finally, Experiment C was designed to illustrate the effect of global mechanisms and again, it was confirmed.

On the other hand, all three experiments were very special. They were precisely designed to emphasize desired characteristics. In reality it is not the case. For example when a biological cell passes a narrow channel or a vessel, it deforms in an unpredictable way. The $\mathcal{F}$-metrics as demonstrated above, show the ability to draw conclusions about the interplay between different elastic moduli. And all this without prior classification of the actual deformation of the cell.

- $\mathcal{F}$-metrics as a suitable energy-like characteristic of action of elastic forces on the object
- possibility of monitoring local strain (niekde by sa hodil farebny obrazok takej flakatej gule alebo bunky - mozno naozaj len screenshot zo simulacie, kde sa pretlaca cez kanal s tym, ze je v plane spravit detailnejsiu analyzu) - k poslednej odrazke - obrazok by som tam uz nedaval. plan prace sa dava do prezentacii, do clankov az tak velmi nie, aspon mam ten dojem. Mozno sa to moze slovne popisat s nejakym dovetkom, ze to sluzi na analysu lokalnych stresov a pod. A navyse, zda sa mi, ze ten clanok je celkom dobry, normalne sa mi zacina pacit

References

[1] R. Maniyeri, Y. K. Suh, S. Kang, and M. J. Kim, "Numerical study on the propulsion of a bacterial flagellum in a viscous fluid using an immersed boundary method," *Computers & Fluids*, vol. 62, pp. 13–24, Jun. 2012.

[2] A. Gilmanov and F. Sotiropoulos, "A hybrid cartesian/immersed boundary method for simulating flows with 3D, geometrically complex, moving bodies," *Journal of Computational Physics*, vol. 207, no. 2, pp. 457–492, Aug. 2005.

[3] J. Chen, J. Li, and Y. Sun, "Microfluidic approaches for cancer cell detection, characterization, and separation," *Lab on a Chip*, vol. 12, no. 10, pp. 1753–1767, Apr. 2012.

[4] M. Dupin, I. Halliday, C. Care, and L. Alboul, "Modeling the flow of dense suspensions of deformable particles in three dimensions," *Phys Rev E Stat Nonlin Soft Matter Phys.*, vol. 75, p. 066707, 2007.

[5] T. Odenthal, B. Smeets, P. Van Liedekerke, E. Tijskens, H. Van Oosterwyck, and H. Ramon, "Analysis of initial cell spreading using mechanistic contact formulations for a deformable cell model," *PLoS Comput Biol*, vol. 9, no. 10, p. e1003267, 10 2013. [Online]. Available: http://dx.doi.org/10.1371/journal.pcbi.1003267

[6] I. Jančigová and R. Tóthová, "Scalability of forces in mesh-based models of elastic objects," 2014, preprint.

[7] I. Cimrák, M. Gusenbauer, and T. Schrefl, "Modelling and simulation of processes in microfluidic devices for biomedical applications," *Computers and Mathematics with Applications*, vol. 64, no. 3, pp. 278 – 288, 2012.

[8] D. A. Fedosov, B. Caswell, and G. E. Karniadakis, "A multiscale red blood cell model with accurate mechanics, rheology, and dynamics," *Biophysical Journal*, vol. 98, no. 10, pp. 2215–2225, 2010.

[9] ——, "Systematic coarse-graining of spectrin-level red blood cell models," *Computer Methods in Applied Mechanics and Engineering*, vol. 199, no. 29–32, pp. 1937–1948, 2010.

[10] I. Cimrák, M. Gusenbauer, and I. Jančigová, "An ESPResSo implementation of elastic objects immersed in a fluid," *Computer Physics Communications*, vol. 185, no. 3, pp. 900 – 907, 2014.

[11] A. Arnold, O. Lenz, S. Kesselheim, R. Weeber, F. Fahrenberger, D. Roehm, P. Košovan, and C. Holm, "ESPResSo 3.1 - molecular dynamics software for coarse–grained models," in *Meshfree Methods for Partial Differential Equations VI, Lecture Notes in Computational Science and Engineering*, M. Griebel and M. Schweitzer, Eds., vol. 89, 2013, pp. 1–23.

[12] A. Henderson, "ParaView guide, A Parallel Visualization Application," Kitware Inc., Tech. Rep., 2007.